Contribution from the Department of Chemistry,
The Ohio State University, Columbus, Ohio 43210

Borohydride Complexes of Europium(II) and Ytterbium(II) and Their Conversion to Metal Borides. Structures of $(L)_4Yb[BH_4]_2$ (L = CH_3CN, C_5H_5N)

James P. White III, Haibin Deng, and Sheldon G. Shore*

Received January 15, 1991

The borohydride complexes of divalent lanthanides $(CH_3CN)_4Yb[(\mu\text{-}H)_3BH]_2$ (**1**), $(C_5H_5N)_4Yb[BH_4]_2\cdot 2C_5H_5N$ (**2**), $(CH_3CN)_2Eu[BH_4]_2$ (**3**), and $(C_5H_5N)_{1.8}Eu[BH_4]_2$ (**4**) have been prepared, isolated, and characterized. Complexes **1** and **2** have been structurally characterized. Complex **1** consists of two borohydride ligands bound to Yb(II) through three Yb-H-B bridges with a B-Yb-B angle of 103.2°. The CH_3CN ligands are in a "seesaw" arrangement. Crystal data for **1**: space group $C2/c$, monoclinic, a = 13.902 (2) Å, b = 9.431 (1) Å, c = 14.937 (3) Å, β = 124.83 (2) °, V = 1608 (17) Å^3, mol wt = 366.94 g·mol^{-1}, d(calcd) = 1.516 g·cm^{-3} for Z = 4, μ = 58.0 cm^{-1} for Mo Kα radiation. A total of 1875 unique reflections were collected at −50 °C over the range $4 \le 2\theta \le 55°$ with 1623 reflections having $I \ge 3\sigma(I)$ used in the final refinement. R_F = 0.021 and R_{wF} = 0.028. Octahedral coordination geometry is observed in complex **2**. The borohydride ligands are trans to each other with a crystallographically imposed B-Yb-B angle of 180°. Although B-H hydrogen atoms were not located, the borohydride ligands are believed to be bound to Yb(II) through three Yb-H-B bridge bonds. The pyridine ligands are disordered but are resolved to give two enantomeric molecules, in which the pyridines are arranged in the shape of "four-bladed right- and left-handed propellers", with the nitrogens, para carbons, and the lanthanide metal all coplanar. Crystal data for **2**: space group $C2/m$, monoclinic, a = 15.511 (2) Å, b = 11.594 (1) Å, c = 11.649 (2) Å, β = 131.73 (1)°, V = 1563.4 (4) Å^3, mol wt = 677.34 g·mol^{-1}, d(calcd) = 1.439 g·cm^{-3} for Z = 2, μ = 30.084 cm^{-1} for Mo Kα radiation. A total of 1463 unique reflections were collected at −50 °C over the range $4 \le 2\theta \le 50°$ with 1463 reflections having $I \ge 3\sigma(I)$ used in the final refinement. R_F = 0.022 and R_{wF} = 0.034. The bonding in these complexes is predominantly ionic, with metal-ligand distances in the range of those observed previously. Complexes **1** and **3** were thermally decomposed to give lanthanide borides.

Introduction

Borohydride complexes of numerous metal ions are known.[1-3] Of the lanthanide elements, the trivalent lanthanide complexes $Ln[BH_4]_3$ (Ln = Sm, Eu, Gd, Tb, Dy, Ho, Er, Tm, Yb, Lu),[4] $LnCl[BH_4]_2$ (Ln = Y, Sm, Gd, Ho, Dy), and $LnCl_2[BH_4]$ (Ln = Sm, Er, Yb) have been prepared,[5] as well as several $Cp_2Ln[BH_4]\cdot n$THf (Ln = Sm, Er, Yb; n = 0, 1) compounds.[6] No complete structural characterization has been reported for these lanthanide borohydrides, although a borohydride complex of the pseudo-lanthanide Y(III), $(THF)_3Y[BH_4]_3$, has been prepared and structurally characterized.[7] Two analogous lanthanide complexes, $Ln[BH_4]\cdot 3$THF (Ln = Er, Gd), are believed to be isostructural with the Y(III) complex, while the lanthanide(III) borohydride apppears to be different; only their unit cell dimensions have been determined.[8] Borohydride complexes of tetravalent Ce, $Cp_3Ce[BH_4]$ and $(\text{indenyl})_2Ce[BH_4]_2$, are known,[9] but borohydride complexes of the Ln(II) ions (Ln = Sm, Eu, Yb) have not been reported. We have undertaken the syntheses and characterization of $Ln[BH_4]_2$ complexes, as an extension of our study of low-valent lanthanide compounds.[10a,b]

We have found that acetonitrile and pyridine are exceptionally good ligands for Ln(II) ions.[10b] They promote formation of complexes with boron hydride and carborane anions.[10a,11] Use of these amines allows isolation of complexes that would otherwise be insoluble or unstable in other solvents. When these amines are employed as solvents, stable lanthanide(II) borohydride complexes can be isolated.

Reported herein are the syntheses and coordination chemistry of a series of europium(II) and ytterbium(II) borohydride complexes (**1-4**) and the structural characterization of two ytterbium borohydride complexes, $(CH_3CN)_4Yb[(\mu\text{-}H)_3BH]_2$ (**1**) and $(C_5H_5N)_4Yb[BH_4]_2\cdot 2C_5H_5N$ (**2**). Complex **2** is a tetragonally distorted octahedron with trans $[BH_4]^-$ groups and represents the first example of a linear anion-Ln-anion bonding arrangement for an Ln(II) compound. The borohydride complexes are relatively stable in solution but slowly decompose via loss of coordinated ligands and H_2 as solids. This instability has been exploited by using these compounds as precursors to lanthanide borides. By thermal decomposition of **1** and **3**, YbB_4 and EuB_6 were prepared.

Experimental Section

General Data. All manipulations were performed under inert-atmosphere conditions due to the air- and moisture-sensitive nature of Ln(II) compounds. Standard vacuum-line and inert-atmosphere techniques were employed.[12] Acetonitrile (Mallinckrodt) was stirred over P_2O_5 for 10 days before being distilled for use. Pyridine (Fisher) was dried and distilled from Na immediately prior to use. Hexanes (Baker) were stirred over H_2SO_4 for 2 days, washed with H_2O, dried with CaH_2, and then distilled from Na before use. NH_3 (Matheson) was distilled from Na immediately prior to use. NH_4Cl (Fisher) was recrystallized from anhydrous methanol and vacuum dried at 120 °C prior to use. Yb metal (Strem), Sm metal (Strem), and $Na[BH_4]$ (Fisher) were used as received. Eu ingot (Strem) was obtained packed in oil. It was washed with hexanes to remove any oil and then cut into strips (ca. 100 mg).

All IR spectra were recorded with 2-cm^{-1} resolution by using a Mattson-Polaris FT-IR spectrometer. NMR spectra were obtained by using a Brucker MSL-300 spectrometer with a boron-free probe equipped for heteronuclear decoupling, operating at 96.3 MHz (^{11}B, $\delta(BF_3\cdot OEt_2)$ = 0.00 ppm) and 300 MHz (^{1}H, δ(TMS) = 0.00 ppm).

Single-crystal X-ray diffraction data were collected with an Enraf-Nonius CAD4 diffractometer. Computations were carried out on PDP 11/44 and DEC Vax station 3100 computers, using the SDP structure determination package.[13] All data were corrected for Lorentz and polarization effects, decay, and absorption (empirically from ψ-scan data). The lanthanide positions were determined from Patterson maps or by using the direct-method MULTAN 11/82. Remaining atoms were located and the structures were solved by a combination of the direct-method MULTAN 11/82 and difference Fourier techniques with analytical

(1) James, B. D.; Wallbridge, M. G. H. *Prog. Inorg. Chem.* **1970**, *11*, 99.
(2) Gilbert, K. B.; Boocock, S. K.; Shore, S. G. *Comprehensive Organometallic Chemistry*, Wilkinson, G., Stone, F. G. A., Abel, E., Eds.; Pergamon Press: London, 1982, pp 879-945.
(3) Marks, T. J.; Kolb, J. R. *Chem. Rev.* **1977**, *77*, 263.
(4) Zange, E. *Chem. Ber.* **1960**, *93*, 652.
(5) Rossmanith, K.; Macalka, H. *Monatsh. Chem.* **1963**, *94*, 295.
(6) Marks, T. J.; Grynkewich, G. W. *Inorg. Chem.* **1976**, *15*, 6, 1302.
(7) Segal, G. B.; Lippard, S. G. *Inorg. Chem.* **1978**, *17*, 844.
(8) Bernstein, E. R.; Chen, K. M. *Chem. Phy.* **1975**, *10*, 215.
(9) Kapur, S.; Kalsotra, B. L.; Multani, R. K.; Jain, B. D. *J. Inorg. Nucl. Chem.* **1973**, *35*, 1689.
(10) (a) White, III, J. P.; Deng, H.-B.; Shore, S. G. *J. Am. Chem. Soc.* **1989**, *111*, 8946. (b) White, III, J. P. Ph.D. Dissertation, The Ohio State University, 1990.
(11) Manning, M. J.; Knobler, C. B.; Hawthorne, M. F. *J. Am. Chem. Soc.* **1988**, *110*, 4458.
(12) Shriver, D. F.; Drezdzon, M. A. *The Manipulation of Air Sensitive Compounds*; John Wiley & Sons: New York, 1969.
(13) SDP (developed by B. A. Frenz and Associates, Inc., College Station, TX 77840) was used to process X-ray data, to apply corrections, and to solve and refine the structures.

0020-1669/91/1330-2337$02.50/0

scattering factors used throughout. Full-matrix least-squares refinements were employed. Powder X-ray data were collected on a Scintag PAD-5 powder X-ray diffractometer. The diffractometer was interfaced with a Data General computer, which contained a JCPDS library file for identification of diffraction patterns.[24]

The following metathesis reactions all employ the appropriate lanthanide dichlorides as starting materials, synthesized according to a preparation[14] in the literature, with the modifications listed below.

$(CH_3CN)_4Yb[(\mu\text{-}H)_3BH]_2$ (1). In a drybox a 50-mL flask containing a Teflon-coated magnetic stir bar was charged with 130 mg (0.751 mmol) of Yb metal and 79.2 mg (1.48 mmol) of NH_4Cl. The flask was connected to a vacuum-line extractor, which was then evacuated. Dry NH_3 (20 mL, liquid) was condensed in the flask at −196 °C, and the flask was warmed to −33 °C and stirred. An immediate reaction occurred with evolution of H_2 as the NH_3 melted. With increasing H_2 pressure, the reaction slowed appreciably. To increase the reaction rate, the solution was frozen twice at −196 °C and H_2 was removed. After 40 min, H_2 evolution ceased and a golden yellow suspension was present. Solvent NH_3 was removed, resulting in a green NH_3-solvated solid, $(NH_3)_xYbCl_2$. Dry CH_3CN (5 mL) was condensed into the flask at −78 °C. The CH_3CN displaced coordinated NH_3 upon warming. Solvent was pumped away, and treatment with CH_3CN was repeated. Light green $(CH_3CN)_xYbCl_2$ was present in the flask upon removal of the solvent for a second time. The flask was then charged with 54.9 mg (1.45 mmol) of $NaBH_4$ in a drybox and again evacuated. Next, 20 mL of dry CH_3CN was condensed into the flask at −78 °C, and the mixture was warmed to room temperature and stirred. Some H_2 formed as the system warmed up. After 10 min, the mixture was cooled to −78 °C and the H_2 was pumped away. The solution was then warmed to room temperature and stirred for 3 h. During this time, the solution turned orange in color with white and dark green precipitates forming. Filtration of the reaction mixture yielded a bright orange filtrate of $(CH_3CN)_xYb[BH_4]_2$. Cooling this filtrate to 0 °C with slow removal of the CH_3CN solvent under vacuum yielded orange X-ray-quality crystals of **1**. Removal of all the solvent at room temperature gave an orange-yellow solid, which became bright yellow $(CH_3CN)_2Yb[BH_4]_2$ after washing with hexanes and vacuum drying. A yield of 157 mg of **1** (76% based on $NaBH_4$) was obtained. Anal. Calcd for $C_4H_{14}N_2YbB_2$: C, 16.87; H, 4.95; N, 9.84. Found: C, 16.14; H, 4.89; N, 9.53. Infrared spectrum (Nujol, NaCl plates; cm^{-1}): ν_{B-H} 2363 (s, sh), 2310 (vs), 1176 (s), 1109 (s); $\nu_{C\equiv N}$ 2271 (vs), 2265 (vs); ν_{Yb-H-B} 1604 (vw, br). Infrared spectrum (CH_3CN, NaCl plates; cm^{-1}): ν_{B-H} 2377 (s), 2214 (vs), 1160 (m), 1094 (m); ν_{Yb-H-B} 1604 (vw, br). ^{11}B NMR spectrum (CD_3CN, 303–225 K): −32.5 ppm (quintet, J_{B-H} = 80 Hz). ^1H NMR spectrum (CD_3CN, 303 K): 0.30 ppm (quartet, J_{B-H} = 78 Hz).

$(C_5H_5N)_4Yb[BH_4]_2\cdot 2C_5H_5N$ (2). In a drybox a 50-mL flask containing a Teflon-coated magnetic stir bar was charged with 125 mg (0.722 mmol) of Yb metal and 76.2 mg (1.42 mmol) of NH_4Cl. The flask was connected to a vacuum-line extractor, which was then evacuated, and then $(NH_3)_xYbCl_2$ was prepared in the same manner as described for **1** above. Dry C_5H_5N (5 mL) was condensed into the flask at −78 °C (ca. 5 mL). The pyridine immediately displaced coordinated NH_3 upon warming the reaction flask. The solvent was removed and the treatment with C_5H_5N was repeated, with the isolation of deep violet $(C_5H_5N)_xYbCl_2$ upon removal of the solvent. The flask was then charged with 53.5 mg (1.41 mmol) of $NaBH_4$ in a drybox and again evacuated. Next, 20 mL of dry C_5H_5N was condensed into the flask at −78 °C, and the mixture was warmed to room temperature and stirred. The solution turned a deep violet color as soon as the pyridine melted. A small amount of H_2 formed upon warming the reaction flask. After 10 min, the mixture was cooled to −78 °C and the H_2 was pumped away. The solution was again warmed to room temperature and stirred for 2 h. Filtration of the reaction mixture yielded a deep violet filtrate of $(C_5H_5N)_xYb[BH_4]_2$. Cooling this filtrate to 0 °C with slow removal of the pyridine solvent under vacuum yielded violet, X-ray-quality crystals of $(C_5H_5N)_4Yb[BH_4]_2\cdot 2C_5H_5N$. Removal of all the solvent at room temperature and washing once with hexanes gave a dark violet solid of approximate composition $(C_5H_5N)_{2.75}Yb[BH_4]_2$, which became a rust-colored solid of approximate formula $(C_5H_5N)_{1.5}Yb[BH_4]_2$ after repeated washings with hexanes and vacuum drying. A yield of 247 mg of violet solid (83% based on $NaBH_4$) was obtained. Anal. Calcd for $C_{55}H_{87}N_{11}Yb_4B_8$: C, 39.30; H, 5.22; N, 9.17. Found: C, 39.38; H, 4.30; N, 8.66. Infrared spectrum (Nujol, NaCl plates; cm^{-1}): ν_{B-H} 2390 (s, sh); 2360 (vs), 2342 (vs); 2337 (vs); 2248 (s); 2216 (s); ν_{Yb-H-B} 1948 (vw); 1930 (vw); 1876 (vw); 1869 (vw); $\nu_{C=C}$ 1596 (vs, s). ^{11}B NMR spectrum (C_5D_5N, 303–225 K): −32.4 ppm (quintet, J_{B-H} = 81 Hz). ^1H NMR spectrum (C_5D_5N, 303 K): 2.26 ppm (s, br).

$(CH_3CN)_2Eu[BH_4]_2$ (3). In a drybox a 50-mL flask containing a Teflon-coated magnetic stir bar was charged with 128 mg (0.842 mmol) of Eu metal and 89 mg (1.66 mmol) of NH_4Cl. The flask was connected to a vacuum-line extractor, which was then evacuated. CH_3CN-solvated $EuCl_2$ was prepared in a procedure identical with that used for the Yb analogue described for **1** above. The flask was then charged with 60 mg (1.59 mmol) of $NaBH_4$ in a drybox and again evacuated. Next 20 mL of dry CH_3CN was condensed into the flask at −78 °C, and the mixture was warmed to room temperature and stirred. Some H_2 formed as the flask warmed to room temperature, mostly due to a reaction with the small quantity of black precipitate. After 10 min, the mixture was cooled to −78 °C and the H_2 was pumped away. The solution was then warmed to room temperature and stirred for 3 h. During this time, the solution turned bright yellow-green while white and black precipitates formed. Filtration of the reaction mixture yielded a brilliant yellow-green filtrate of $(CH_3CN)_xEu[BH_4]_2$. Removal of all the solvent at room temperature gave a yellow-green solid that became a light yellow powder of $(CH_3CN)_2Eu[BH_4]_2$ after it was washed with hexanes and vacuum dried. A yield of 97 mg (42% based on $NaBH_4$) of **3** was obtained. Anal. Calcd for $C_4H_{14}N_2EuB_2$: C, 18.22; H, 5.35; N, 10.62. Found: C, 17.02; H, 5.62; N, 10.41. Infrared spectrum (Nujol, NaCl plates; cm^{-1}): ν_{B-H} 2390 (s, sh), 2301 (vs); $\nu_{C\equiv N}$ 2280 (vs, sh), 2268 (vs); ν_{Eu-H-B} 1604 (w, br).

$(C_5H_5N)_{1.8}Eu[BH_4]_2$ (4). In a drybox a 50-mL flask containing a Teflon-coated magnetic stir bar was charged with 143 mg (0.941 mmol) of Eu metal and 99.5 g (1.86 mmol) of NH_4Cl. Yellow $(C_5H_5N)_3EuCl_2$ was then prepared in the same manner as described for the Yb analogue in **2** above. The flask containing $(C_5H_5N)_3EuCl_2$ was then charged with 69.0 mg (1.82 mmol) of $NaBH_4$ in a drybox and again evacuated. Next 20 mL of dry C_5H_5N was condensed into the flask at −78 °C, and the mixture was warmed to room temperature and stirred. Some H_2 formed as the flask warmed to room temperature. After 10 min, the mixture was cooled to −78 °C and the H_2 was pumped away. The solution was then warmed to room temperature and stirred for 2 h. During this time, the solution turned red-orange in color with white and black precipitates forming. Filtration of the reaction mixture yielded a red-orange filtrate of $(C_5H_5N)_xEu[BH_4]_2$. Removal of all the solvent at room temperature gave **4**, a canary yellow powder after washing with hexanes and vacuum drying. A yield of 228 mg (74% based on $NaBH_4$) was obtained. Anal. Calcd for $C_{45}H_{85}N_9Eu_5B_{10}$: C, 33.36; H, 5.29; N, 7.78. Found: C, 33.01; H, 3.97; N, 7.67. Infrared spectrum (Nujol, NaCl plates; cm^{-1}): ν_{B-H} 2371 (vs), 2316 (s); 2275 (m, sh); 2249 (s), 2185 (m); ν_{Eu-H-B} 2005 (vw); 1992 (vw); 1946 (vw); 1929 (vw); 1888 (vw); 1869 (vw); $\nu_{C=C}$ 1595 (vs, s). Anal. Calcd for $C_{15}H_{15}N_3EuCl_2$: C, 39.15; H, 3.29; N, 9.13. Found: C, 38.53; H, 3.16; N, 8.85.

YbB_4. Complex **1** was vacuum dried. In the drybox, the resulting yellow powder was loaded into a 15-mm-diameter quartz tube fitted with a vacuum-line adaptor. The flask was evacuated to 10^{-5} Torr and then heated in a tube furnace to 1000 °C over a 1-h period. A −196 °C trap was placed in series with the reaction vessel to collect any condensible gases evolved. At ca. 100 °C CH_3CN evolved, followed by evolution of H_2 from 150 to 200 °C. Between 350 and 500 °C Yb metal sublimed from the tube and condensed on the walls of the tube immediately outside the furnace. No further volatiles were emitted from the tube up to 1000 °C. The tube was cooled to room temperature, and shiny gray YbB_4 was removed from the tube. Powder X-ray revealed that small amounts of Yb_2O_3 were present in the solid. Washing the solid with 1 M HCl completely removed the oxide impurity. Powder X-ray data for YbB_4 (d, Å (I) for Cu Kα): 4.015 (46), 3.540 (33), 3.163 (71), 2.653 (54), 2.510 (32), 2.482 (92), 2.233 (16), 2.119 (15), 2.004 (17), 1.951 (20), 1.848 (17), 1.741 (15), 1.713 (28), 1.691 (27), 1.662 (13), 1.575 (44), 1.535 (17), 1.332 (8), 1.300 (24), 1.280 (13), 1.247 (9), 1.227 (11) 1.2009 (10), 1.158 (14).

EuB_6. In a manner analogous to that used to prepare YbB_4 above, complex **3** was thermally decomposed, with CH_3CN, H_2, and Eu vapor forming at approximately the same temperatures. The maximum temperature of the decomposition was 700 °C. Broad bands in the powder X-ray pattern indicate the EuB_6 is not yet fully crystalline. No other phases were observed.

X-ray Structure Determination for $(CH_3CN)_4Yb[(\mu\text{-}H)_3BH]_2$ (1). Single crystals of the air-sensitive compound were isolated in a solvent-saturated N_2 atmosphere and sealed in thin-walled glass capillaries. Lattice parameters were determined from 25 reflections ($24° \le 2\theta \le 30°$). Crystal data are listed in Table I.

The diffraction symmetry (C_{2h}, $2/m$) and the systematic absences (hkl for $h + k = 2n + 1$, $h0l$ for $h, l = 2n + 1$) are consistent with either the centrosymmetric space group $C2/c$ or the noncentrosymmetric space group Cc. Diffraction statistics favor $C2/c$. The structure was solved in this space group. Attempted solution of the structure in Cc gave a clearly unreasonable result. The position of the Yb atom was determined directly from the initial difference map and refined to convergence. All

(14) Howell, J. K.; Pytlewski, L. L. *J. Less-Common Met.* **1969**, *18*, 437.

Table I. Crystallographic Data for $(CH_3CN)_4Yb[(\mu\text{-}H)_3BH]_2$ and $(C_5H_5N)_4Yb[BH_4]_2\cdot 2C_5H_5N$

chem formula	$C_8H_{20}N_4YbB_2$	$C_{30}H_{38}N_6YbB_2$
fw	366.94	677.34
space group	$C2/c$ (No. 15)	$C2/m$ (No. 12)
a, Å	13.902 (2)	15.511 (2)
b, Å	9.431 (1)	11.594 (1)
c, Å	13.937 (3)	11.649 (2)
β, deg	124.83 (2)	131.73 (1)
V, Å^3	1608	1563.3
Z	4	2
d(calcd), g·cm^{-3}	1.516	1.439
temp, °C	−50	−50
radiation (λ, Å)	Mo Kα(0.710 73)	Mo Kα(0.710 73)
μ, cm^{-1}	58.0	30.08
transm coeff	0.691–1	0.724–0.999
$R(R_o)$	0.021	0.022
$R_w(F_o)$	0.028	0.034

other heavy atoms were then located and refined isotropically. A full anisotropic refinement of all heavy atoms allowed location of all the hydrogen atoms from the resulting difference map. Except for one methyl hydrogen, all H positional and thermal parameters were fully refined. The final refinement of all atoms produced a difference map with residual electron density <0.34 e/Å^3 except for two ghost peaks within 0.9 Å of Yb.

X-ray Structure Determination for $(C_5H_5N)_4Yb[BH_4]_2\cdot 2C_5H_5N$ (2). Single crystals of the air-sensitive compound were mounted in thin-walled glass capillaries in a solvent-saturated N_2 atmosphere and then sealed. Lattice parameters were determined from 25 reflections ($24° \le 2\theta \le 30°$). Crystal data are given in Table I.

The diffraction symmetry (C_{2h}, $2/m$) and the systematic absences (hkl for $h + k = 2n + 1$, $h0l$ for $h = 2n + 1$) are consistent with either the noncentrosymmetric space groups $C2$ and Cm or the centrosymmetric space group $C2/m$. Diffraction statistics marginally favor the noncentrosymmetric space groups. Solution of the structure in these three space groups gives essentially the same structure: Four pyridines and two borons in octahedral coordination with Yb(II). The boron atoms are trans to each other and the nitrogens and para carbons of the pyridines are in the equatorial plane. The pyridine rings were thus pitched with respect to the B–Yb–B axis and form a four-bladed propeller geometry. There are two pyridines of solvation in the lattice.

In space group $C2$, the pyridine ligands are well-behaved, but the positions of the two boron atoms oscillate with respect to the Yb atom, located at the origin (0, 0, 0), and cannot be refined to convergence. This suggests that the two boron atoms are related by a mirror plane at $y = 0$. This additional symmetry element is present in the $C2/m$ and Cm space groups. Furthermore, the two pyridine molecules of solvation appear to be related by a mirror plane at $y = 0$. When the boron positions were fixed and all the heavy atoms were refined anisotropically, all the pyridine hydrogens except those on the para carbons of the pyridines of solvation could be located. No hydrogens around the boron could be located, and a final agreement factor of $R = 0.035$ was obtained. In the space groups Cm and $C2/m$ the crystallographically unique boron position refines to convergence. However, pyridine ligands are disordered due to the presence of the mirror plane at $y = 0$, producing two orientations for each ring, due to reflection of the ortho and meta carbons across the plane. These carbons were refined at $^1/_2$ weight. $R_F = 0.037$ for Cm and $R_F = 0.022$ for $C2/m$.

Space group $C2/m$ was chosen for the final refinement of the structure, since it gives the lowest agreement factor and space group Cm offers no advantages. Refinement of the crystallographically unique pyridine molecule of solvation gave unacceptably high thermal parameters and some of the atoms would not refine to convergence. By assignment of a weight of $^1/_2$ to the pyridine atoms, reasonable thermal parameters were obtained and all of the atoms refined. Thus, it apppears that two pyridines of solvation are distributed among the four available equivalent positions in the unit cell.

In the final refinements all of the heavy atoms were fully refined anisotropically. Pyridine hydrogen positions were then calculated for a distance of $r_{C-H} = 0.95$ Å and given thermal parameters $B(H) = (B(C) + 1)$ Å^2. A para hydrogen was not assigned to the pyridine of solvation, because the presence of a hydrogen on both the nitrogen and para carbon atoms suggested that there is also a slight head-to-tail disorder in the lattice pyridines. All heavy atoms were then refined to convergence with the hydrogen positions fixed. New hydrogen positions were then calculated, and this procedure was repeated until the heavy-atom positions refined to convergence. The resulting difference map showed a 1.2 e/Å^3 ghost peak 0.1 Å from B, but no other residual electron density peaks above 0.3 e/Å^3 were observed. No definite positions for the $[BH_4]^-$ hydrogens could be located.

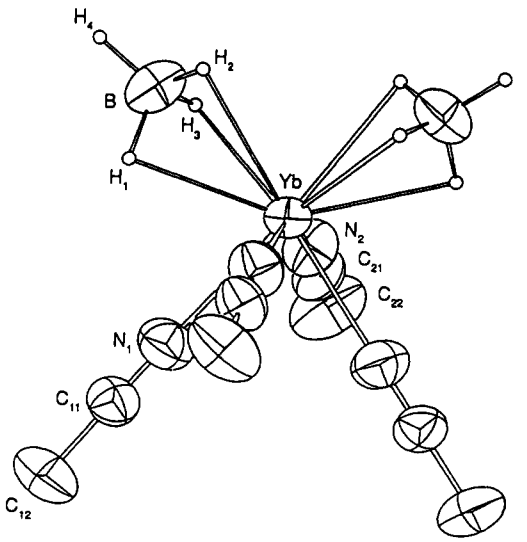

Figure 1. Molecular structure of $(CH_3CN)_4Yb[(\mu\text{-}H)_3BH]_2$ (**1**), with 50% thermal ellipsoids. Methyl hydrogens are not shown.

Table II. Selected Bond Distances and Angles and Their Esd's for $(CH_3CN)_4Yb[(\mu\text{-}H)_3BH]_2$

Bond Distances, Å			
Yb–N1	2.529 (4)	B–H1	1.19 (7)
Yb–N2	2.520 (3)	B–H2	1.05 (6)
Yb–B	2.666 (6)	B–H3	1.09 (5)
		B–H4	1.07 (9)
Yb–H1	2.46 (6)		
Yb–H2	2.52 (6)	N1–C11	1.118 (5)
Yb–H3	2.33 (5)	C11–C12	1.444 (6)
		N2–C12	1.135 (5)
		C12–C22	1.443 (6)
Bond Angles, deg			
N1–Yb–N2	78.1 (1)	H1–B–H2	94 (4)
N1–Yb–B	90.9 (2)	H1–B–H3	110 (4)
N2–Yb–B	97.5 (2)	H1–B–H4	113 (6)
		H2–B–H3	109 (5)
B–Yb–B′	103.2	H2–B–H4	115 (6)
N1–Yb–N1	75.0	H3–B–H4	114 (5)
N2–Yb–N2	152.5		
		Yb–N1–C11	170.5 (4)
Yb–H1–B	87 (3)	N1–C11–C12	179.4 (5)
Yb–H2–B	86 (4)		
Yb–H3–B	95 (4)	Yb–N2–C21	170.7 (4)
		N2–C21–C22	179.4 (6)

Results and Discussion

Syntheses. The bis(borohydride) complexes **1–4** were synthesized via the route shown in eq 1. The reactions were carried

$$L_xLnCl_2 + 2Na[BH_4] \xrightarrow[-NaCl]{L} L_xLn[BH_4]_2 \qquad (1)$$

$$L = CH_3CN,\ C_5H_5N;\ Ln = Eu,\ Yb$$

out in acetonitrile and in pyridine from which the soluble complexes were isolated. The reactions were most rapid when C_5H_5N is the solvent, probably because the lanthanide dichlorides are very soluble in this solvent. The C_5H_5N–bis(borohydride) complexes are stable in solution; however, the CH_3CN complexes slowly decompose upon standing. All the complexes are unstable as solids and will lose some coordinated solvent, change color, and slowly evolve H_2 when stored in vacuum or under dry nitrogen at room temperature. Colors of the complexes (in their corresponding solvents), orange (**1**), violet (**2**), yellow (**3**), and red-orange (**4**), are the same as those observed for the Yb(II) and Eu(II) $[B_{10}H_{10}]^{2-}$ and $[B_{10}H_{14}]^{2-}$ complexes in these solvents.[10a,b]

Structure of $(CH_3CN)_4Yb[(\mu\text{-}H)_3BH]_2$ (1). The molecular structure of **1** is shown in Figure 1. Selected bond distances and angles are given in Table II. Positional parameters are listed

Table III. Positional Parameters and Their Esd's for $(CH_3CN)_4Yb[(\mu\text{-}H)_3BH]_2$

atom	x	y	z	B, Å²
Yb	1.000	0.14781 (2)	0.250	3.221 (4)
N1	1.1343 (4)	0.3606 (3)	0.3114 (4)	5.6 (1)
N2	1.0275 (3)	0.2112 (4)	0.4271 (2)	4.95 (8)
C11	1.1911 (3)	0.4563 (4)	0.3494 (3)	4.43 (8)
C12	1.2634 (4)	0.5809 (5)	0.3977 (3)	5.8 (1)
C21	1.0387 (3)	0.2583 (5)	0.5024 (3)	4.54 (8)
C22	1.0518 (5)	0.3190 (6)	0.5975 (3)	7.0 (1)
B	1.1820 (4)	−0.027 (5)	0.3320 (4)	5.4 (1)
H1	1.204 (4)	0.077 (6)	0.385 (4)	6 (1)
H2	1.124 (4)	−0.067 (5)	0.349 (4)	5 (1)
H3	1.132 (3)	0.000 (5)	0.246 (3)	4 (1)
H4	1.275 (5)	−0.093 (9)	0.359 (6)	9 (2)
H11	1.289 (4)	0.586 (6)	0.474 (4)	5 (1)
H12	1.296 (5)	0.616 (6)	0.366 (5)	5 (1)
H13[a]	1.352	0.555	0.457	4
H21	1.075 (6)	0.392 (7)	0.610 (6)	9 (2)
H22	0.976 (8)	0.325 (9)	0.568 (8)	13 (4)
H23	1.060 (5)	0.246 (9)	0.638 (5)	8 (2)

[a] H13 was located but not refined.

Table IV. Selected Bond Distances and Angles and Their Esd's for $(C_5H_5N)_4Yb[BH_4]_2\cdot 2C_5H_5N$

	Bond Distances, Å		
Yb–N1	2.566 (3)	N2–C6	1.322 (8)
Yb–N2	2.579 (4)	C6–C7	1.39 (1)
Yb–B	2.692 (4)	C7–C8	1.35 (1)
N1–C1	1.332 (6)	C8–C9	1.34 (1)
C1–C2	1.365 (9)	C9–C10	1.39 (1)
C2–C3	1.367 (7)	N2–C10	1.327 (8)
C3–C4	1.369 (7)	N3–C11	1.31 (2)
C4–C5	1.362 (9)	C11–C12	1.37 (1)
N1–C5	1.331 (6)	C12–C13	1.30 (1)
		C13–C14	1.29 (1)
		C14–C15	1.37 (1)
		N3–C15	1.32 (2)
	Bond Angles, deg		
N1–Yb–N2	89.96 (1)	Yb–N2–C6	122.0 (4)
N1–Yb–B	90.00	Yb–N2–C10	121.8 (4)
N2–Yb–B	90.00	N2–C6–C7	123.3 (8)
B–Yb–B′	180	C6–C7–C8	119.5 (8)
N1–Yb–N1′	180	C7–C8–C9	118.2 (6)
N2–Yb–N2′	180	C8–C9–C10	120.0 (8)
		C9–C10–N2	122.8 (8)
Yb–N1–C1	122.0 (3)	C6–N2–C10	116.2 (6)
Yb–N1–C5	122.1 (3)		
N1–C1–C2	123.8 (5)	C13–C14–C15	123.2 (8)
C1–C2–C3	119.1 (5)	C14–C15–N3	116.2 (9)
C2–C3–C4	118.1 (5)	C15–N3–C11	123 (1)
C3–C4–C5	119.2 (5)	N3–C11–C12	116.9 (9)
C4–C5–N1	123.9 (5)	C11–C12–C13	122.4 (8)
C1–N1–C5	116.0 (4)	C12–C13–C14	118.0 (6)

in Table III. The molecule has crystallographically imposed $C2$ point symmetry.

Each borohydride unit is bound to ytterbium through three Yb–H–B bridges. The B–Yb–B angle involving the borohydride ligands with respect to the central ytterbium atom is 103.2°. This angle is significantly smaller than the (cp centroid)–Yb–(cp centroid) angles observed in ytterbium(II) bis(cyclopentadienide) complexes, which range from 114° in $(MeC_5H_4)_2Yb(THF)$[15] to 144° in $(C_5Me_5)_2Yb(THF)\cdot 0.5CH_3C_6H_5$.[16] The three bridging hydrogens of **2** have Yb–H distances of 2.33 (5), 2.46 (6), and 2.52 (6) Å. The average Yb–H distance is 2.4 (1) Å, not significantly different from the 2.3 (1) Å average observed in $(CH_3CN)_6Yb[\mu\text{-}H)_2B_{10}H_{12}]\cdot 2CH_3CN$.[10a] The Yb–B distance of 2.666 (6) Å for the η^3 mode of $[BH_4]^-$ in **1** is, however, significantly shorter than the 2.84 (4) Å observed for the closest Yb–B distance in $(CH_3CN)_6Yb[(\mu\text{-}H)_2B_{10}H_{12}]\cdot 2CH_3CN$.[10a]

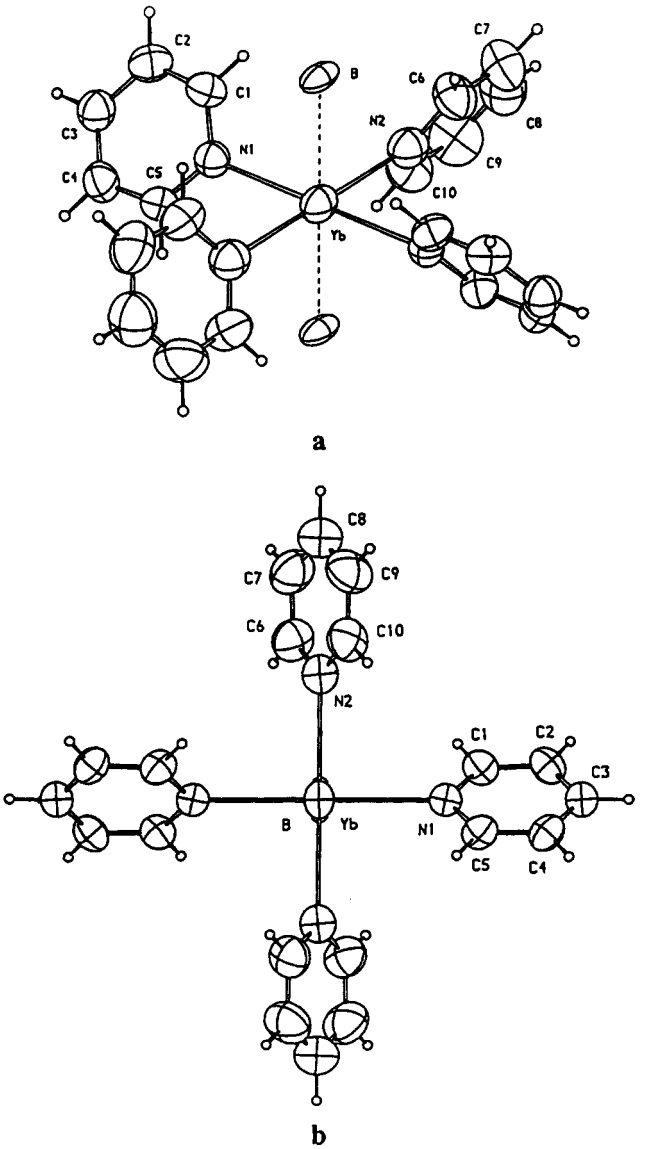

Figure 2. (a) Molecular structure of $(C_5H_5N)_4Yb[BH_4]_2$ (**2**), with 50% thermal ellipsoids. (b) Molecular structure of **2** viewed down the crystallographic C_2 axis.

The four acetonitrile ligands in **1** are arranged in a "seesaw" configuration with respect to the central ytterbium atom. There is a single 2-fold axis, which bisects the B–Yb–B and N–Yb–N angles. The N–Yb–N bond angles for the symmetry-equivalent nitrogen atoms are 152.5 and 75.0° for N1 and N2, respectively. The Yb–N bond distances have average values of 2.525 (9) Å, in good agreement with the average distance of 2.54 (9) Å observed in $(CH_3CN)_6Yb[(\mu\text{-}H)_2B_{10}H_{12}]\cdot 2CH_3CN$.[10a] The acetoniitrile ligands are linear, with an average N–C–C bond angle of 179.4 (6)°, but the Yb–N–C angles are slightly bent with an average bond angle of 170.4 (4)°. Slightly bent acetonitrile ligands on Yb(II) were also observed in $(CH_3CN)_6Yb[(\mu\text{-}H)_2B_{10}H_{12}]$,[10a] which has an average Yb–N–C angle of 171 (2)° for linear (N–C–C_{av} = 178 (2)°) acetonitrile ligands.

Structure of $(C_5H_5N)_4Yb[BH_4]_2\cdot 2C_5H_5N$ (2). The molecular structure of **2** consists of an axially distorted octahedral arrangement of ligands around Yb(II). Borohydride ligands are trans to each other along the elongated axis. Nitrogens, para carbons, and para hydrogens of the bound pyridines are coplanar with the Yb cation, in the equatorial plane of the octahedron. Due to the presence of the crystallographic mirror plane, there are two possible orientations for each of the four pyridine ligands. This disorder is most easily resolved by assuming the presence of a racemic mixture of enantiomers in the unit cell in which the

(15) Zinnen, H. A.; Pluth, J. J.; Evans, W. J. *J. Chem. Soc., Chem. Commun.* **1980**, 810.
(16) Tilley, T. D.; Anderson, R. A.; Spencer, B.; Ruben, H.; Zalkin, A.; Templeton, D. H. *Inorg. Chem.* **1980**, *19*, 2999.

Table V. Positional Parameters and Their Esd's for $(C_5H_5N)_4Yb[BH_4]_2 \cdot 2C_5H_5N$

atom	x	y	z	B,[a] Å²
Yb	0.000	0.000	0.000	3.946 (5)
B1	0.000	0.2322 (4)	0.000	3.77 (8)
N1	0.1653 (3)	0.000	−0.0002 (3)	3.62 (8)
C1	0.2493 (4)	0.0785 (6)	0.0769 (6)	4.0 (1)
C2	0.3389 (5)	0.0815 (6)	0.0800 (7)	4.4 (1)
C3	0.3442 (3)	0.000	0.0001 (4)	4.3 (1)
C4	0.2586 (5)	−0.0813 (6)	−0.0802 (6)	4.3 (1)
C5	0.1725 (5)	−0.0784 (6)	−0.0770 (5)	4.0 (1)
N2	−0.1482 (3)	0.000	−0.2966 (4)	4.7 (1)
C6	−0.1529 (6)	0.0842 (8)	−0.3771 (8)	5.7 (2)
C7	−0.2309 (7)	0.086 (1)	−0.5367 (8)	6.8 (2)
C8	−0.3084 (6)	0.000	−0.6162 (6)	7.1 (2)
C9	−0.3062 (7)	−0.085 (1)	−0.537 (1)	6.9 (3)
C10	−0.2246 (6)	−0.0844 (8)	−0.3771 (8)	5.7 (2)
H1	0.2468	0.1357	0.1329	5*
H2	0.3966	0.1394	0.1368	5*
H3	0.4056	0.000	0.000	5*
H4	0.2593	−0.1391	−0.1374	5*
H5	0.1139	−0.1357	−0.1330	5*
H6	−0.1002	0.1466	−0.3299	7*
H7	−0.2295	0.1473	−0.5895	8*
H8	−0.3632	0.000	−0.7253	9*
H9	−0.6303	−0.1468	−0.5899	8*
H10	−0.2235	−0.1466	−0.3231	7*
N3	0.1037 (8)	0.250 (1)	0.7076 (9)	8.6 (3)
C11	0.0281 (8)	0.333 (1)	0.6361 (8)	7.0 (3)
C12	−0.0486 (7)	0.3312 (8)	0.4785 (9)	6.1 (2)
C13	−0.0490 (6)	0.2499 (6)	0.4025 (5)	4.7 (2)
C14	0.0276 (7)	0.1690 (7)	0.4788 (8)	6.0 (2)
C15	0.1096 (9)	0.166 (1)	0.6358 (9)	7.1 (3)
H11	0.0264	0.3927	0.6907	9*
H12	−0.1037	0.3916	0.4233	7*
H14	0.0274	0.1087	0.4233	7*
H15	0.1653	0.1070	0.6900	9*

[a] Asterisks indicate calculated atom positions and thermal parameters; $B(H) = B(C) + 1$.

pyridine ligands are arranged in the shape of "four-bladed right- and left-handed propellers". The molecular structure is shown in Figure 2a. Another view of **2** projected down the B–Yb–B "propeller shaft" is shown in Figure 2b. Selected bond distances and angles are given in Table IV. Positional parameters are listed in Table V.

The Yb–N distances in **2** are 2.566 (5) and 2.579 (4) Å for N1 and N2, respectively, with an average value of 2.572 (5) Å. These distances compare favorably with the average Yb–N distances of 2.57 (1) and 2.565 Å observed in the Yb(II) complexes $(COT)Yb(C_5H_5N)_3$ and $(C_5Me_5)_2Yb(C_5H_5N)_2$, respectively.[17,18] Although the B–Yb–B axis is a crystallographically imposed 2-fold axis, it is also a pseudo-4-fold axis, and there are four pseudo-2-fold axes in the equatorial plane. Thus, the molecule approaches D_{4d} point symmetry. The dihedral angle between the pyridine plane containing N1 and the equatorial plane is 53.6°, and the dihedral angle between the pyridine plane containing N2 and the equatorial plane is 60.0°.

The Yb–B distance in **2** of 2.692 (5) Å is slightly longer than the 2.666 (6) Å distance in **1**, but the difference is not statistically significant. A Yb–B distance similar to that in **1** would suggest that the bonding mode of $[BH_4]^-$ in **2** should be similarly η^3, since metal–boron distances are observed to increase upon decreasing hapticity of the borohydride ligand.[3] Unfortunately, hydrogens on the borohydride could not be located to verify this possibility. The difficulty in locating hydrogens may be caused by the disordered nature of the molecular packing. However, usually a larger difference in the metal–B bond is observed for different coordination modes of $[BH_4]^-$. For example, in $U[BH_4]_4$, which has both tridentate and bidentate borohydrides,[19] the difference

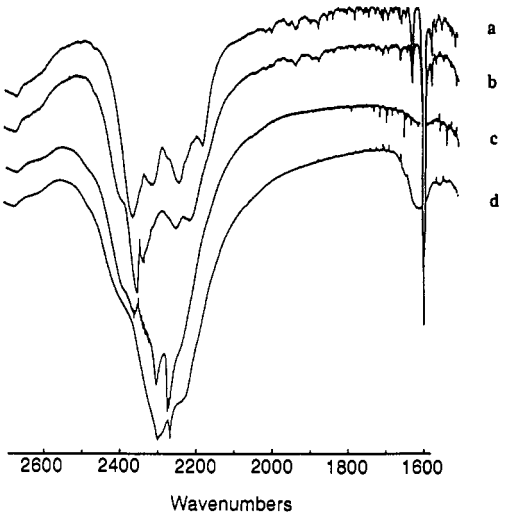

Figure 3. IR spectra in Nujol of complexes in the B–H and Ln–H–B regions: (a) $(C_5H_5N)_{1.5}Yb[BH_4]_2$ (**2**); (b) $(C_5H_5N)_{1.8}Eu[BH_4]_2$ (**4**); (c) $(CH_3CN)_2Yb[BH_4]_2$ (**1**); (d) $(CH_3CN)_2Eu[BH_4]_2$ (**3**).

in U–B distances for these two coordination modes is 0.38 Å, much larger than the 0.03-Å difference between **1** and **2**. Thus, although the X-ray data cannot be used to determine the true binding mode of the borohydride in **2**, the observed Yb–B distance suggests that it is similar to that in **1**.

NMR and IR Spectra. ^{11}B NMR chemical shifts of **1** and **2** in CH_3CN and C_5H_5N solutions are slightly upfield of that of $Na[BH_4]$, and the ^{11}B–^1H coupling constants of **1** and **2** are in excellent agreement with the reported value for this salt.[20] The ^{11}B NMR signals of **1** and **2** are quintets down to −48 °C, the lowest temperature accessible in the solvents employed. This apparent equivalence of B–H hydrogens is due to their fluxional character, which is observed for nearly all metal–borohydride complexes on the ^{11}B NMR time scale.[21] The proton NMR spectra of **1** show a broad 1:1:1:1 quartet centered at 0.3 ppm, while no B–H coupling is observed in the spectrum of **2**, which shows only a broad singlet at 2.25 ppm. The downfield shift of the protons in **2** versus those in **1** is probably due to the different ligands on the Yb(II). The IR spectra, in Nujol, of **1**–**4** in the B–H and Ln–H–B regions are shown in Figure 3. The absorptions agree well with the predicted positions for η^3-bound borohydride.[6] Two of the B–H terminal absorptions for complex **2** are shifted slightly from those of **1**, possibly due to differences of the amine ligands. The similarity of the two spectra in this region lend support to the assumption that the coordination modes of the borohydride ligands in **1** and **2** are the same. In addition to these bands, some very weak absorptions from 2000 to 1600 cm^{-1} are observed. The CH_3CN complexes **1** and **3** show a single broad band at ca. 1600 cm^{-1}. The band is much more prominent in the spectrum of **3**. The C_5H_5N complexes **2** and **4** show a series of three weak doublets from 2000 to 1850 cm^{-1}. These absorptions are of equal intensity in both the Eu(II) and Yb(II) spectra. These weak absorptions are probably due to Yb–H–B stretches.[3,6]

Formation of Lanthanide Borides. The borohydride complexes of Ln(II) are unstable as dry solids. Removal of solvent from these complexes causes an irreversible reaction to occur over time, either in vacuum or under dry nitrogen, concomitant with evolution of H_2. This instability was observed for $[B_{10}H_{14}]^{2-}$, $[B_{10}H_{13}]^-$, and $[B_{10}H_{15}]^-$ complexes of Eu(II) and Yb(II) as well.[10b] This was particularly true for the CH_3CN complexes. Upon redissolution of complexes **1** and **3** that have been dry for some time, noticeable amounts of H_2 are evolved. The ^{11}B spectrum of the resulting solution of **1** in CH_3CN showed numerous unassignable boron

(17) Wayda, A. L.; Mukerji, I.; Dye, J. L.; Rogers, R. D. *Organometallics* **1987**, *6*, 1328.
(18) Tilley, T. D.; Anderson, R. A.; Brock, S.; Zalkin, A. *Inorg. Chem.* **1982**, *21*, 2647.
(19) Bernstein, E. R.; Keiderling, T. A.; Lippard, S. J.; Mayerle, J. J. *J. Am. Chem. Soc.* **1972**, *94*, 2552.
(20) Onak, T. P.; Landesman, H.; Williams, R. E.; Shapiro, I. *J. Phys. Chem.* **1959**, *63*, 1533.
(21) Kennedy, J. D. *Prog. Inorg. Chem.* **1984**, *32*, 519.

resonances, along with signals due to the original compound. If complexes **1** and **3** are heated in vacuum at 200 °C, CH_3CN and H_2 are evolved (eq 2). Nujol IR spectra of the resulting solids

$$(CH_3CN)_xLn[BH_4]_2 \xrightarrow[-CH_3CN,\ -H_2]{200\ °C,\ vacuum} \text{"}LnB_2\text{"} \qquad (2)$$

Ln = Eu, Yb

reveal no B-H or ligand stretches, indicating they contain only Ln and B. These solids represent an intimate mixture of elemental lanthanide and boron in a precise 1:2 ratio, an ideal starting point for producing a metal boride. To investigate this further, dry solids from complexes **1** and **3** solids were heated in a quartz tube maintained at 10^{-5} Torr to a maximum of 1000 °C over the period of 1 h (eqs 3 and 4). At 100 °C coordinated solvent is evolved,

$$(CH_3CN)_xYb[BH_4]_2 \xrightarrow[-CH_3CN,\ -H_2,\ -Yb]{1000\ °C,\ vacuum} YbB_4 \qquad (3)$$

$$(CH_3CN)_xEu[BH_4]_2 \xrightarrow[-CH_3CN,\ -H_2,\ -Eu]{7000\ °C,\ vac} EuB_6 \qquad (4)$$

and hydrogen evolution is observed above 150 °C. Above 450 °C, lanthanide metal was observed to sublime out of both compounds. The resulting materials were shiny gray solids with a metallic luster. Powder X-ray data revealed they were single-phase crystalline YbB_4 and EuB_6 from complexes **1** and **3**, respectively.[24]

The formation of EuB_6 was not surprising, since the binary phase diagram for these elements indicates that the hexaboride is the only stable boride phase.[22] The formation of YbB_4 was unusual, however, since a stable YbB_2 phase is known but none was formed.[23] There are also stable YbB_6 and YbB_{12} phases known, but none of the more boron-rich species were formed either. Obviously, under the reaction conditions the metal-rich boride is unstable, losing metal to give the observed tetraboride. An X-ray powder pattern of EuB_6 prepared at 700 °C shows that it is not yet fully crystalline but still identifiable as EuB_6. The X-ray powder pattern of YbB_4 prepared at 1000 °C shows that it is fully crystalline. There was a slight contaminant of Yb_2O_3 in the YbB_4, presumably from the quartz tube. Washing the boride with dilute HCl completely removed the oxide impurity, confirmed by the absence of oxide peaks in powder X-ray patterns of the washed material.

Conclusions

Borohydride complexes of Eu(II) and Yb(II) can be synthesized by using C_5H_5N and CH_3CN as solvents. The amines ligate the lanthanide ions, and isolable coordination complexes are formed. The borohydride complexes are unstable as solids, particularly the CH_3CN complexes, which are easily decomposed to form single crystalline phase europium and ytterbium borides.

Acknowledgment. For support of this work we thank the Army Research Office for Grant DAAL03-88-K-0176 and the National Science Foundation for an X-ray diffractometer through Grant 84-11630. NMR spectra were obtained at The Ohio State University Campus Chemical Instrument Center funded in part by NSF Grant 79-10019 and NIH Grant 1 S10 PR0140518-01A. We thank Mr. Patrick Clark for obtaining and reading X-ray powder photographs.

Supplementary Material Available: Listings of crystal data, anisotropic thermal parameters, bond distances, and bond angles (5 pages); listings of calculated and observed structure factor amplitudes (19 pages). Ordering information is given on any current masthead page.

(22) *Binary Alloy Phase Diagrams*; Massalski, T. B., Ed.; American Society for Metals: Metals Park, OH, 1986; Vol. 1, p 354.
(23) Reference 22, p 398.
(24) *Powder Diffraction File: Inorganic Phases*; McClune, W. F., Ed.; JCPDS (Joint Committee on Powder Diffraction Standards) International Center for Diffraction Data: Swarthmore, PA, 1989.

Contribution from the Department of Chemistry and Biochemistry, University of Colorado, Boulder, Colorado 80309

New Classes of Skeletally Stabilized Tri- and Tetraphosphazanes

Joseph M. Barendt,[1] R. Curtis Haltiwanger, Christopher A. Squier, and Arlan D. Norman*

Received January 4, 1991

Reactions of 1,2,4,5-$(NH_2)_4C_6H_2$ with $(Et_2N)_3P$ and 1,2,3-$(NH_2)_3C_6H_3$ with $(Me_2N)_3P$ yield the new bis(triphosphazane) $C_6H_2[N_2[P(NEt_2)_2]_2PNEt_2]_2$ (**4**) and tetraphosphazane $C_6H_3N_3[P(NMe_2)_2]_2(PNMe_2)_2$ (**6**), respectively. **4** with sulfur is oxidized at the exo phosphorus atoms to a tetrasulfide $C_6H_2[N_2[P(S)(NEt_2)_2]_2PNEt_2]_2$ (**5**). **6** reacts with elemental selenium to form stepwise diselenide $C_6H_3N_3[P(Se)(NMe_2)_2]_2(PNMe_2)_2$ (**7**) and tetraselenide $C_6H_3N_3[P(Se)(NMe_2)_2]_2[P(Se)NMe_2]_2$ (**8**). **6** with elemental sulfur yields directly the tetrasulfide $C_6H_3N_3[P(S)(NMe_2)_2]_2[P(S)NMe_2]_2$ (**10**). **7** reacts smoothly with anhydrous HCl to yield the dichloride $C_6H_3N_3[P(Se)(NMe_2)_2]_2(PCl)_2$ (**9**); in contrast, **4**-**6** with HCl undergo extensive cleavage with skeletal unit destruction. **4**-**10** have been characterized by spectral (^1H and ^{31}P NMR, MS, and IR) data. **4**, **8**, and **10** have also been characterized in the solid by single-crystal X-ray diffraction. Crystal data for **4**: monoclinic, $P2_1/c$, a = 12.573 (3) Å, b = 16.976 (3) Å, c = 15.455 (3) Å, β = 111.55 (2)°, V = 3068(5) Å^3, Z = 2, d_{calc} = 1.12 g cm^{-3}, R = 0.055, and R_w = 0.085. Crystal data for **8**: orthorhombic, *Pbca*, a = 14.858 (3) Å, b = 21.626 (6) Å, c = 22.327 (7) Å, V = 7174 (3) Å^3, Z = 8, d_{calc} = 1.68 g cm^{-3}, R = 0.060, and R_w = 0.076. Crystal data for **10**: orthorhombic, *Pbca*, a = 14.706 (3) Å, b = 21.610 (5) Å, c = 22.000 (5) Å, V = 6991 (3) Å^3, Z = 8, d_{calc} = 1.20 g cm^{-3}, R = 0.049, and R_w = 0.050. **6** contains the longest linear extension of a P(III) phosphazane system so far achieved, the result of skeletal stabilization of the phosphazane system. **4** contains a near-planar $P_2N_4C_6$ atom core with two 1,3,2-diazaphosphole rings incorporated at the 1,2- and 4,5-positions of a benzene ring. **8** and **10** contain a planar $P_2N_3C_6$ atom core consisting of two fused 1,3,2-diazaphosphole rings attached at the 1,2,3-positions of a benzene ring. Structural features of **4** and **5** and the **6**-**10** series are compared and discussed.

Introduction

The location of *o*-phenylene groups between adjacent nitrogen atoms of a phosphazane skeleton in order to achieve skeletal stabilization (**1**) has been used for synthesis of a variety of new phosphorus(III) phosphazane oligomers[2-6] and polymers.[5-7] With

(1) Present address: Callery Chemical Co., P.O. Box 429, Pittsburgh, PA 15230.
(2) (a) Barendt, J. M.; Haltiwanger, R. C.; Norman, A. D. *J. Am. Chem. Soc.* **1986**, *108*, 3127. (b) Barendt, J. M.; Haltiwanger, R. C.; Norman, A. D. *Inorg. Chem.* **1988**, *28*, 2334.

0020-1669/91/1330-2342$02.50/0